JOURNAL OF SPACECRAFT AND ROCKETS
Vol. 29, No. 4, July–August 1992

Solar Sail Halo Orbits II: Geocentric Case

Colin R. McInnes* and John F. L. Simmons†
University of Glasgow, Glasgow G12 8QQ, Scotland, United Kingdom

The equations of motion of a geocentric orbiting high-performance solar sail are analyzed in a corotating reference frame with the axis of corotation directed along the Sun-Earth line. Stationary solutions are found to the equations of motion in the corotating frame that correspond to Earth-centered halo-type orbits when viewed from an inertial frame. The sail performance requirements are minimized and families of linearly stable trajectories identified. By patching these halo orbits together, it will be shown that complex new trajectories may be formed. Geocentric halo orbits may have useful space science and technology applications.

Nomenclature

a, a_j, a = radiation pressure acceleration vector, acceleration components, Keplerian ellipse semimajor axis
C_j = numerical constants ($j = 1,5$)
e = Keplerian ellipse eccentricity
$F_{1,2}$ = transfer functions, Eq. (48)
i = Keplerian ellipse ecliptic inclination
k = axis of off-axis halo orbit
l = direction of incident radiation along Sun-line
M_1, M = gyroscopic matrix and gravity gradient tensor $\{U_{ij}\}$
n = sail orientation vector
O = remaining terms of order greater than
P_o = radiation pressure at 1 AU, 9.13×10^{-6} Nm^{-2}
r, r = sail position vector, $r = |r|$
R_o = planetary radius
t = time variable
U = two-body potential function in corotating frame
u = auxiliary variable, $z^{2/3}$
v = sail velocity vector
z = halo displacement, sail cylindrical coordinate
α = sail orientation with respect to Sun-line
β = sail loading parameter (dimensionless radiation pressure acceleration)
γ_j = coefficients ($j = 1,2$), Eq. (31)
δ = vector perturbation applied to sail ($r \rightarrow r + \delta$)
η = perturbation applied to sail ($z \rightarrow z + \eta$)
θ = sail azimuthal cylindrical coordinate
Λ = auxiliary variable, $\beta^{2/3}$
μ = gravitational parameter, 3.98602×10^5 km^{3}s^{-2}
ξ = perturbation applied to sail ($\rho \rightarrow \rho + \xi$)
ρ = halo amplitude, sail cylindrical coordinate
σ = sail mass per unit area
ϕ = angle between off-axis halo and Sun-line, $\cos^{-1}\{l \cdot k\}$
Φ = cone angle of halo, $\tan^{-1}\{\rho/z\}$
Φ_2 = two-body potential function ($-\mu/r$)
ψ = centrifugal potential
Ψ = perturbation applied to sail ($\theta \rightarrow \theta + \Psi$)
ω, ω_j = frequencies of eigenmodes of perturbation
Ω, Ω, Ω_* = angular velocity vector of corotating frame, $\Omega = |\Omega|$, $\Omega_* = \mu r^{-3/2}$
∇ = cylindrical polar gradient operator $\{\partial/\partial\rho, (1/\rho)(\partial/\partial\theta), \partial/\partial z\}$

Subscripts

1 = with respect to initial halo
2 = with respect to final halo
a = evaluated at apogee
m = maximum value of a variable
o = evaluated at a fixed operating point
p = evaluated at perigee

Received June 5, 1990; revision received Dec. 10, 1990; accepted for publication Dec. 15, 1990.

*Lecturer in Space Systems, Department of Aerospace Engineering.
†Lecturer in Astronomy, Department of Physics and Astronomy.

Introduction

FOLLOWING the heliocentric halo orbit case,[1,2] another new mode of operation of solar sails is now discussed, that of geocentric halo orbits. By suitably choosing the sail parameters and orientation, it will be found that it is possible to displace a solar sail in a near-polar orbit above the planetary terminator in the anti-Sun direction (Fig. 1), with the sail orbital period, halo amplitude ρ, and displacement distance z chosen at will. The dynamical model assumes a uniform radiation field over the scale of the problem (tens of planetary radii), so that the ratio of the radiation pressure acceleration to the local gravitational acceleration increases with increasing distance from the planetary center. It is this relation that leads to interesting new dynamics. The region of space over which the assumptions remain valid will, however, be limited, due to solar/lunar perturbations. Given that the lunar mean sphere of influence has a radius of order $10R_o$, we will consider halo orbits with a geocentric distance of up to 40–$50R_o$. Over this distance, the solar radiation pressure varies by only 4×10^{-3} from the value at 1 AU. The analysis is, of course, invalid along the planetary shadow near $\rho = 0$.

The sail orbital period may be chosen to be synchronous with a Keplerian near-polar orbit of radius equal to the halo amplitude, fixed at some particular value for all (ρ,z), or, with a suitable choice of orbital period, the requirements on the sail

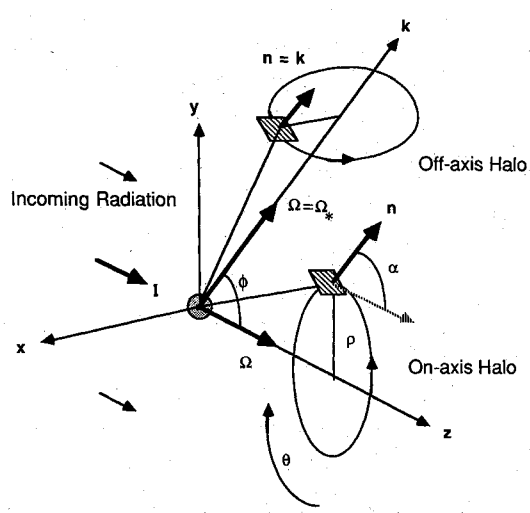

Fig. 1 Geometry of geocentric halo orbits.

loading parameter may be minimized. Furthermore, for this minimal loading family of orbits, the axis of the halo need not lie along the Sun-Earth line (Fig. 1). The dynamical stability of the various orbits is investigated, and it will be shown that linearly stable families of halo orbits exist. By patching together individual halo orbits, it will also be shown that complex new trajectories may be formed by a simple switching of the sail orientation at discrete points along the orbit.

Dynamical Equations and Their Solution

We consider now the equations of motion for a perfectly reflecting, plane, and homogeneous solar sail in a corotating reference frame, with the origin centered on a point mass Earth and the axis of rotation Ω directed along the Sun-Earth line (Fig. 1). The sail orientation is given by a unit vector $\boldsymbol{n}$ fixed in the corotating frame, and the magnitude of the solar radiation pressure acceleration is given by the parameter $\beta = P_o/\sigma$, where P_o is the solar radiation pressure acceleration at 1 AU and σ is the total sail mass per unit area. Since the sail orientation is fixed in the corotating frame, the sail must rotate once per orbit with respect to an inertial frame.

In this first-order analysis, we will neglect the rotation of the Sun-Earth line, since the inertial forces introduced by further rotating the coordinate system with the Sun-Earth line are small with respect to the large radiation pressure force required to establish the halo orbits. It will be assumed that the effect of these inertial forces may be corrected through active control of the sail orientation.

The vector equation of motion for a solar sail in the corotating frame, under the action of a point mass potential and superimposed uniform radiation field, is given by

$$\frac{d^2\boldsymbol{r}}{dt^2} + 2\boldsymbol{\Omega} \times \frac{d\boldsymbol{r}}{dt} + \boldsymbol{\Omega} \times (\boldsymbol{\Omega} \times \boldsymbol{r}) = \boldsymbol{a} - \nabla \Phi_2(|\boldsymbol{r}|) \tag{1}$$

The gravitational potential $\Phi_2(|\boldsymbol{r}|)$ and the radiation pressure acceleration $\boldsymbol{a}$ are given by

$$\Phi_2(|\boldsymbol{r}|) = -\mu/|\boldsymbol{r}| \qquad \text{and} \qquad \boldsymbol{a} = \beta(\boldsymbol{l}\cdot\boldsymbol{n})^2\boldsymbol{n} \tag{2}$$

where the unit vector $\boldsymbol{l} = (0,0,1)$ is directed along the assumed fixed Sun-Earth line with the requirement that $\boldsymbol{l}\cdot\boldsymbol{n} \geq 0$. This ensures that the normal to the sail always points away from the Sun and, consequently, constrains the sail motion to the planetary night-side ($+z$). Equation (1) may be simplified by introducing a scalar potential $\psi(\boldsymbol{r})$ to represent the conservative centrifugal term, viz.,

$$\nabla\psi(\boldsymbol{r}) = \boldsymbol{\Omega} \times (\boldsymbol{\Omega} \times \boldsymbol{r}) \tag{3}$$

where $\psi(\boldsymbol{r}) = -\frac{1}{2}|\boldsymbol{\Omega}\times\boldsymbol{r}|^2$. Defining a new potential, $U(\boldsymbol{r}) = \Phi_2(|\boldsymbol{r}|) + \psi(\boldsymbol{r})$, Eq. (1) becomes

$$\frac{d^2\boldsymbol{r}}{dt^2} + 2\boldsymbol{\Omega} \times \frac{d\boldsymbol{r}}{dt} + \nabla U(\boldsymbol{r}) = \boldsymbol{a} \tag{4}$$

In the corotating frame, we require stationary solutions, so that the first two terms in Eq. (4) vanish. Since the vector $\boldsymbol{a}$ is oriented in direction $\boldsymbol{n}$, taking the vector product of $\boldsymbol{n}$ with Eq. (4), it is found that

$$\nabla U(\boldsymbol{r}) \times \boldsymbol{n} = 0 \Rightarrow \boldsymbol{n} = \lambda \nabla U(\boldsymbol{r}) \tag{5}$$

where λ is an arbitrary scalar multiplier. Using the normalization condition, $|\boldsymbol{n}| = 1$, we identify λ as $|\nabla U(\boldsymbol{r})|^{-1}$, so that the sail orientation required for stationary solutions in the corotating frame is given by

$$\boldsymbol{n} = \frac{\nabla U(\boldsymbol{r})}{|\nabla U(\boldsymbol{r})|} \tag{6}$$

Since we have uniform corotation, there can be no azimuthal component of the radiation pressure acceleration, so that the vector $\boldsymbol{n}$ must lie in the plane perpendicular to the sail velocity vector. The sail orientation may then be described by a single angle α between $\boldsymbol{l}$ and $\boldsymbol{n}$, where α is defined by

$$\tan\alpha = \frac{|\boldsymbol{l}\times\boldsymbol{n}|}{\boldsymbol{l}\cdot\boldsymbol{n}} \tag{7}$$

Furthermore, we may obtain the radiation pressure acceleration required by taking a scalar product of $\boldsymbol{n}$ with Eq. (4). Again requiring stationary solutions in the corotating frame and substituting for $\boldsymbol{n}$, we obtain

$$\beta = \frac{|\nabla U(\boldsymbol{r})|^3}{(\nabla U(\boldsymbol{r})\cdot\boldsymbol{l})^2} \tag{8}$$

In geocentric cylindrical polar coordinates (ρ,θ,z), the corotating potential may be written as

$$U(\rho,z) = -\left[\frac{1}{2}(\Omega\rho)^2 + \frac{\mu}{r}\right], \qquad r^2 = \rho^2 + z^2 \tag{9}$$

Therefore, evaluating the potential gradient, we obtain from Eqs. (7) and (8) scalar expressions for the sail orientation and radiation pressure acceleration required for a halo orbit of amplitude ρ, displacement z, and period $2\pi/\Omega$:

$$\tan\alpha(\rho,z;\Omega) = \left(\frac{\rho}{z}\right)\left[1 - \left(\frac{\Omega}{\Omega_*}\right)^2\right], \qquad \Omega_*{}^2 = \mu/r^3 \tag{10a}$$

$$\beta(\rho,z;\Omega) = \Omega_*{}^2\left\{1 + \left(\frac{\rho}{z}\right)^2\left[1 - \left(\frac{\Omega}{\Omega_*}\right)^2\right]^2\right\}^{3/2} z \tag{10b}$$

where Ω_* is the angular velocity of a Keplerian orbit of radius r. The case of $\Omega = 0$ corresponds to the static equilibrium "Statite" concept[3] for low bit rate communications with high-latitude regions. The sail then simply "levitates" above the Earth, the radiation pressure force exactly balancing the gravitational force with $\beta = \mu/z^2$, as discussed by Forward[3] using the same dynamical model. If we choose the unit of length to be the planetary radius R_o and choose $\mu = 1$, then the parameter β will be the sail radiation pressure acceleration made dimensionless with respect to the gravitational acceleration at R_o. This will now be termed the sail loading parameter.

Polar Synchronous Mode

For polar synchronism, we will choose the sail orbital period $2\pi/\Omega$ to be equal to that of a Keplerian near-polar orbit above the planetary terminator, with an orbital radius equal to the halo amplitude ρ (i.e., $\Omega = \rho^{-3/2}$). Thus, the sail will maintain polar synchronism at all displacement distances z, and we will have cylindrical surfaces of corotation (equal orbital period) extending in the anti-Sun direction. The equatorial inclination of the Keplerian orbit will vary from 66.5 deg at the solstices to 90 deg at the equinoxes. From Eqs. (10), we obtain the required sail orientation and loading:

$$\tan\alpha(\rho,z) = \left\{\frac{\rho}{z}\right\}\left\{1 - \left[1 + \left(\frac{z}{\rho}\right)^2\right]^{3/2}\right\} \tag{11a}$$

$$\beta(\rho,z) = \frac{z}{r^3}\left\{1 + \left\{\frac{\rho}{z}\right\}^2\left[1 - \left(1 + \left\{\frac{z}{\rho}\right\}^2\right)^{3/2}\right]^2\right\}^{3/2} \tag{11b}$$

A section of the surfaces (of revolution) of constant sail loading generated by Eq. (11b), along with the required sail orientations for polar synchronism, are shown in Fig. 2. The relation between the sail loading parameter and the total sail mass per unit area required is given in the appendix for halo orbits about various bodies. It can be seen that, for reasonably low sail loadings, halo orbits of large amplitude with respect

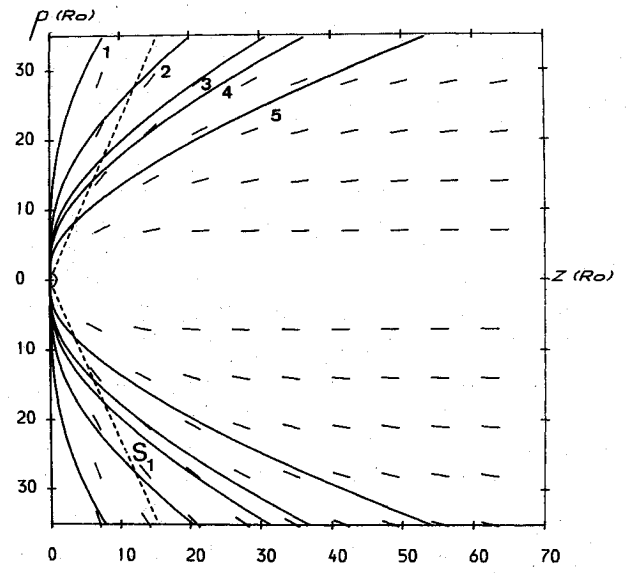

Fig. 2 Polar synchronous surfaces. Loading values of 1) 2×10^{-4}, 2) 8×10^{-4}, 3) 2×10^{-3}, 4) 3×10^{-3}, and 5) 9×10^{-3}.

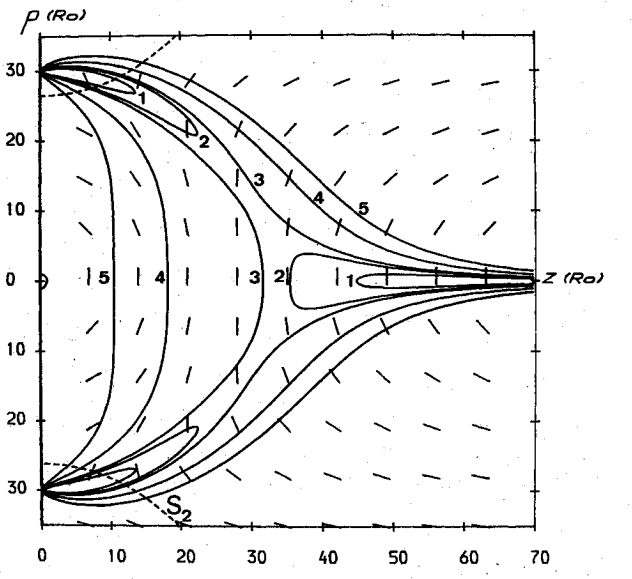

Fig. 3 General synchronous surfaces. Loading values of 1) 5×10^{-4}, 2) 8×10^{-4}, 3) 1×10^{-3}, 4) 3×10^{-3}, and 5) 9×10^{-3}.

to their displacement distance are required. For example, a 5.24-day geocentric halo with a $20R_o$ amplitude and $5R_o$ displacement requires a low sail mass per unit area of 1.33 g^{-2}.

General Synchronous Mode

The sail orbital period may also be chosen to be fixed at some particular value for all displacements and amplitudes. This is equivalent to choosing the period to be synchronous with some particular orbital radius r_o (i.e., $\Omega = r_o^{-3/2}$). From Eqs. (10), we may generate surfaces of constant sail loading, with Ω chosen to be some fixed value. Figure 3 shows a section of these surfaces with the sail orbital period chosen to be synchronous with a Keplerian orbit of radius $30R_o$ (period $\simeq 9.6$ days in the geocentric case). It can be seen that, for lower values of the sail loading, there are two topologically disconnected surfaces that grow and connect.

Optimal Halo Mode

In the previous two sections, the sail orbital period has been chosen to be some particular value to achieve a desired synchronism. If we now treat the sail orbital period as a free parameter of the system, then the sail loading requirements may be minimized with respect to the sail orbital period, for fixed halo amplitude and displacement, to obtain an optimal family of halo orbits, viz.,

$$\frac{\partial \beta(\rho,z;\Omega)}{\partial \Omega} = 0 \Rightarrow \Omega = \Omega_* \tag{12}$$

Thus, for minimization of the sail loading, we require the sail orbital period to be equal to the orbital period of a Keplerian orbit of radius r. With this sail period, the optimized sail loading and required sail orientation are given by

$$\tan \alpha = 0 \tag{13a}$$

$$\beta = z/r^3 \tag{13b}$$

Therefore, a radial ($\alpha = 0$) sail orientation is required for the optimal halo orbits. In fact, with a radial sail orientation, the problem of the general three-dimensional sail motion can be solved in closed form, using parabolic coordinates and applying Hamilton-Jacobi theory.[4] The halo orbits can then be interpreted in terms of intersections of paraboloids.

As before, surfaces of constant sail loading may be generated. If we fix $\beta = \beta_o$, then Eq. (13b) can be inverted to give

$$\rho(z) = \left(\frac{z^{2/3}}{\Lambda} - z^2\right)^{1/2}, \qquad \Lambda = \beta_o^{2/3} \tag{14}$$

which defines a surface of revolution about the z axis. Making the substitution $u = z^{1/3}$ to clear the radical in Eq. (14) we may write

$$\rho^2(u) = u(\Lambda^{-1/2} + u)\,(\Lambda^{-1/2} - u) \tag{15a}$$

and so

$$\begin{aligned} \rho^2(u) = 0 \Rightarrow u = 0 \quad &\text{or} \quad u = \pm\Lambda^{-1/2} \\ \Rightarrow z = 0 \quad &\text{or} \quad z = \Lambda^{-3/4} \end{aligned} \tag{15b}$$

The point $z = \Lambda^{-3/4}$ (i.e., $z = \beta_o^{-1/2}$) corresponds to the sail "levitating," with the radiation pressure acceleration balancing the local gravitational acceleration. The maximum halo amplitude for a fixed sail loading may be obtained from

$$\frac{d\rho(u)}{du} = \frac{(\Lambda^{-1} - 3u^2)}{2(\Lambda^{-1}u - u^3)^{1/2}} = 0$$

$$\Rightarrow u = (3\Lambda)^{-1/2}, \qquad \text{i.e.,} \qquad z_m = (3)^{-3/4}\beta_o^{-1/2} \tag{16}$$

Furthermore, at this extremal value of z we have, from Eq. (14),

$$\rho_m = 2^{1/2}(3)^{-3/4}\beta_o^{-1/2} \tag{17}$$

Thus, the locus of the maxima of halo amplitudes is given by a cone, defined by

$$\rho_m = \sqrt{2}\, z_m \tag{18}$$

Since the sail orbital period is chosen to minimize the sail loading, the sail orbital period will vary at different points on the constant loading surfaces. The surfaces of corotation (equal orbital period) are given by spheres defined by constant Ω_*. The intersection of these corotation surfaces with surfaces of constant loading give regions where sails on minimal loading halo orbits will have the same orbital period. In Fig. 4, sections of surfaces of constant sail loading have been generated. It can be seen that for small displacements the required minimized sail loading varies rapidly for a given halo amplitude. The line S_4 gives the locus of the maxima of these curves, as defined by Eq. (18).

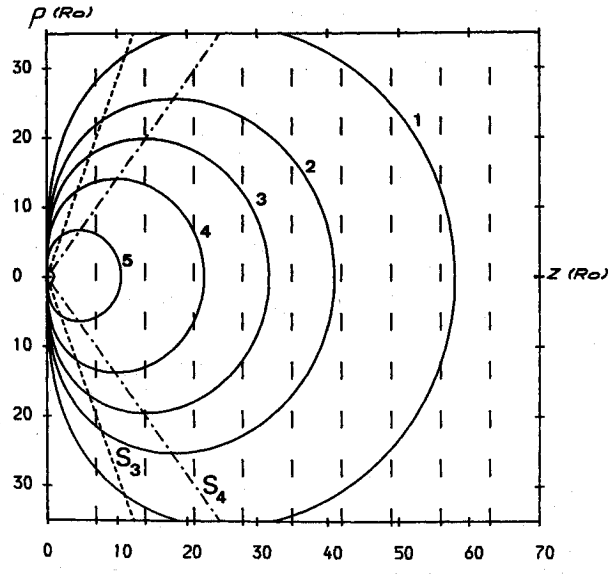

Fig. 4 Minimal loading surfaces. Loading values of 1) 3×10^{-4}, 2) 6×10^{-4}, 3) 1×10^{-3}, 4) 2×10^{-3}, and 5) 9×10^{-3}.

Owing to the radial sail orientation in the minimal loading case, the axis of the halo orbit need not lie along the Sun-line. In fact, any axis k passing through the origin, such that $l\cdot k>0$, will generate new off-axis halo orbits (Fig. 1). The sail loading requirements are, however, increased by a factor $(l\cdot k)^{-2}$, due to the oblique incidence of the photons on the sail while the sail is orientated along the new axis $n=k$.

Using the data in the appendix, it can be seen that, for reasonable values of sail mass per unit area of 1–10 g^{-2}, large-amplitude halo orbits are required for the geocentric case. A 15.38-day optimized geocentric halo with an amplitude of $30R_o$ and displacement of $40R_o$ requires a sail mass per unit area of 2.91 g^{-2}, which is around current attainable values. For halo orbits around other bodies, the requirements on the sail mass per unit area are not so great, even for Mars and especially for Mercury. For the case of Mercury, however, the Sun-planet line rotates rapidly, so that large corrective maneuvers would be required to maintain the halo orbit. Also, as the halo amplitude and displacement increase, solar perturbations become of increasing importance, as do lunar perturbations for the geocentric case. However, with advanced sail materials and designs much tighter and less perturbed, halo orbits would be possible.

Halo Orbit Stability

The dynamical stability of these halo orbits will now be investigated through a linear perturbation analysis and, as will be seen, stable families of halo orbits are found to exist. Since the dynamical model is conservative and there are no dissipative terms, true asymptotic stability is not, in fact, possible. Assuming the sail is at some operating point $r_o=(\rho_o,\theta_o,z_o)$, a perturbation $r_o\rightarrow r_o+\delta$ is applied to Eq. (4) to obtain a variational equation

$$\frac{d^2\delta}{dt^2}+2\Omega\times\frac{d\delta}{dt}+\nabla U(r_o+\delta)-a(r_o+\delta)=0 \tag{19}$$

where $\delta=(\xi,\Psi,\eta)$ represents small displacments in the corotating frame along the (ρ,θ,z) directions. Taylor expanding the potential gradient about the point r_o to first order, we obtain

$$\nabla U(r_o+\delta)=\nabla U(r_o)+\frac{d}{dr}\nabla U(r)\Big|_{r=r_o}+O(|\delta|^2) \tag{20}$$

Then, since $\nabla U(r_o)=a(r_o)$ and the radiation field is uniform, so that $(da/dr)=0$, we obtain a linear variational system

$$\frac{d^2\delta}{dt^2}+M_1\frac{d\delta}{dt}+M\delta=0 \tag{21}$$

where M is the gravity gradient tensor in Eq. (20), and the skew symmetric gyroscopic matrix M_1 is given by

$$M_1=\begin{Bmatrix}0&-2&0\\2&0&0\\0&0&0\end{Bmatrix},\qquad M=\{U_{ij}\}\quad i,j=\rho,\theta,z \tag{22}$$

where U_{ij} is the (i,j) partial derivative of the potential. Since the potential is rotationally symmetric, all partial derivatives with respect to θ vanish. Also, due to the potential being conservative, $M_{31}=M_{13}$. In component form, the variational equations are then

$$\frac{d^2\xi}{dt^2}-2\Omega\rho_o\frac{d\Psi}{dt}+M_{11}\xi+M_{13}\eta=0 \tag{23a}$$

$$\frac{d^2\Psi}{dt^2}+\frac{2\Omega}{\rho_o}\frac{d\xi}{dt}=0 \tag{23b}$$

$$\frac{d^2\eta}{dt^2}+M_{13}\xi+M_{33}\eta=0 \tag{23c}$$

This set of three coupled ordinary differential equations may be reduced by integrating Eq. (23b), viz.,

$$\frac{d\Psi}{dt}=-\frac{2\Omega}{\rho_o}(\xi-\xi_o) \tag{24}$$

which can then be substituted into Eq. (23a). This, then, leads to a constant term $4\Omega^2\xi_o$ in Eq. (23a), which is easily removed by rescaling through a change of variable

$$\xi'=\xi-\frac{4\Omega^2M_{33}}{M_{11}^*M_{33}-M_{13}^2}\xi_o \tag{25a}$$

$$\eta'=\eta+\frac{4\Omega^2M_{13}}{M_{11}^*M_{33}-M_{13}^2}\xi_o \tag{25b}$$

where $M_{11}^*=M_{11}+4\Omega^2$. The resulting set of equations then becomes

$$\frac{d^2}{dt^2}\begin{Bmatrix}\xi'\\\eta'\end{Bmatrix}+\left\{\begin{array}{c:c}M_{11}^*&M_{13}\\\hdashline M_{13}&M_{33}\end{array}\right\}\begin{Bmatrix}\xi'\\\eta'\end{Bmatrix}=0 \tag{26}$$

where the matrix coefficients are given by

$$M_{11}^*=4\Omega^2-\left[\left(\Omega^2-\frac{1}{r^3}\right)+\frac{3\rho^2}{r^5}\right],\qquad M_{13}=-\frac{3\rho z}{r^5}$$
$$M_{31}=M_{13},\qquad M_{33}=\left(\frac{1}{r^3}-\frac{3z^2}{r^5}\right) \tag{27}$$

The stability characteristics of the system will be examined by substituting a solution of the form

$$\begin{Bmatrix}\xi'\\\eta'\end{Bmatrix}=\begin{Bmatrix}\xi_o\\\eta_o\end{Bmatrix}e^{\omega t} \tag{28}$$

which, from Eq. (26), yields

$$\left\{\begin{array}{c:c}\omega^2+M_{11}^*&M_{13}\\\hdashline M_{13}&\omega^2+M_{33}\end{array}\right\}\begin{Bmatrix}\xi_o\\\eta_o\end{Bmatrix}=\begin{Bmatrix}0\\0\end{Bmatrix} \tag{29}$$

For nontrivial solutions, we require that the secular determinant of this matrix equation vanish, viz.,

$$\omega^4 + \gamma_1\omega^2 + \gamma_2 = \prod_{j=1}^{4} (\omega - \omega_j) = 0 \tag{30}$$

where ω_j ($j = 1,4$) are the four frequencies of the eigenmodes of the perturbation. The coefficients of the quartic are given by

$$\gamma_1 = M_{11}^* + M_{33} \tag{31a}$$

$$\gamma_2 = M_{11}^* M_{33} - M_{13}^2 \tag{31b}$$

In general, we will have two pairs of roots, $\omega_{1...4}$, with each pair of opposite sign given by

$$\omega_{1...4} = \pm 2^{-\frac{1}{2}}[-\gamma_1 \pm (\gamma_1^2 - 4\gamma_2)^{\frac{1}{2}}]^{\frac{1}{2}} \tag{32}$$

Therefore, substituting for the coefficients, we obtain

$$\omega_{1...4} = \pm\frac{\Omega_*}{\sqrt{2}}\left(\left[1 - 3\left(\frac{\Omega}{\Omega_*}\right)^2\right] \pm \left\{9\left[1 - \left(\frac{\Omega}{\Omega_*}\right)^2\right]^2 + 36\left(\frac{\Omega}{\Omega_*}\right)^2\left(\frac{z_o}{r_o}\right)^2\right\}^{\frac{1}{2}}\right)^{\frac{1}{2}} \tag{33}$$

The stability of each mode of halo orbit may now be investigated, in turn, by substituting for the required functional form of Ω, and determining the regions where the roots of the characteristic polynomial are real and where they are purely imaginary.

Optimized Halo Mode

For this mode of halo orbit with minimized loading, the sail angular velocity is given by Eq. (12) as $\Omega = \Omega_*$. The roots of the characteristic polynomial then reduce to

$$\omega_{1...4} = \pm\Omega_*\left[-1 \pm 3\left(\frac{z_o}{r_o}\right)\right]^{\frac{1}{2}} \tag{34}$$

For stability, we require that $\omega_j^2 < 0$ ($j = 1...4$), a condition that is always satisfied by the negative root in the bracket and satisfied by the positive root provided that

$$\rho_o > 2\sqrt{2}\, z_o \tag{35}$$

Thus, defining two frequencies Ω_1 and Ω_2 by

$$\Omega_1 = \pm\Omega_*\left[3\left(\frac{z_o}{r_o}\right) - 1\right]^{\frac{1}{2}} \tag{36a}$$

$$\Omega_2 = \pm i\Omega_*\left[3\left(\frac{z_o}{r_o}\right) + 1\right]^{\frac{1}{2}} \tag{36b}$$

we may write

$$\begin{Bmatrix}\xi'\\ \eta'\end{Bmatrix} = \sum_{j=1}^{4}\begin{Bmatrix}\xi_{oj}\\ \eta_{oj}\end{Bmatrix} e^{\omega_j t} \qquad \begin{aligned}\omega_1 &= \Omega_1\\ \omega_2 &= -\Omega_1\\ \omega_3 &= \Omega_2\\ \omega_4 &= -\Omega_2\end{aligned} \tag{37}$$

We, therefore, have a partitioning into two distinct regions of stability and instability, viz.,

1) $\rho_o < 2\sqrt{2}\, z_o$: one real pair of roots ($\omega_{1,2}$) and one purely imaginary pair ($\omega_{3,4}$)—unstable; and

2) $\rho_o > 2\sqrt{2}\, z_o$: two purely imaginary pairs of roots ($\omega_{1...4}$)—stable.

This partitioning is defined by a cone, the section of which is shown in Fig. 4 as S_3. For a given sail loading β, the maximum stable halo displacement and corresponding amplitude are given by

$$z_* = \frac{1}{3\sqrt{3}}\beta^{-\frac{1}{2}}, \qquad \rho_* = \left(\frac{2}{3}\right)^{3/2}\beta^{-\frac{1}{2}} \tag{38}$$

which corresponds to an operating point on the partitioning cone with neutral stability, i.e., $\Omega_1 = 0$. On the cone of maximum halo amplitude, where $\rho = \sqrt{2}\, z$, the shortest time scale of instability is given by Ω_1 as

$$\Omega_1 = \Omega_*(\sqrt{3} - 1)^{\frac{1}{2}} \tag{39}$$

so that the maximum amplitude, minimal loading halo orbit is unstable on a time scale approximately equal to its orbital period.

The coupling of the motion of the halo amplitude perturbations to the azimuthal motion may be found by integrating Eq. (24):

$$\Psi(t) = \Psi_o + \left(\frac{2\Omega\xi_o}{\rho_o}\right)t - \frac{2\Omega}{\rho_o}\int_0^t \xi(t')\, dt' \tag{40}$$

where $\xi(t)$ is given by Eqs. (37) and (25a). The first-order drift in azimuthal position can then be obtained as

$$\Psi(t) = \Psi_o + \left(\frac{2\Omega\xi_o}{\rho_o}\right)\left(1 - \frac{4\Omega^2 M_{33}}{M_{11}^* M_{33} - M_{13}^2}\right)t - \frac{2\Omega}{\rho_o}\sum_{j=1}^{4}\frac{\xi_{oj}}{\omega_j}e^{\omega_j t} \tag{41}$$

For the stable halo orbit families, the azimuthal perturbations are, therefore, in the form of periodic oscillations with a superimposed linear drift. This drift is due to the sail having an initial error in the ρ coordinate, so that the sail has a first-order difference in orbital period from the nominal halo trajectory. The sail is, therefore, constrained to a torus around the nominal halo, and has orbital-type stability.

Polar Synchronous Mode

Substituting for this form of the sail angular velocity the roots of the characteristic equation, as defined by Eq. (32), may be written as

$$\omega_{1...4} = \pm\frac{\Omega_*}{\sqrt{2}}\left(\left[1 - 3\left(\frac{r_o}{\rho_o}\right)^3\right] \pm \left\{9\left[1 - \left(\frac{r_o}{\rho_o}\right)^3\right]^2 + 36\left(\frac{r_o}{\rho_o}\right)^3\left(\frac{z_o}{r_o}\right)^2\right\}^{\frac{1}{2}}\right)^{\frac{1}{2}} \tag{42}$$

Since $\rho_o \le r_o$, the term $1 - 3(r_o/\rho_o)^3 < 0$, so that there will always be at least one pair of stable, purely imaginary roots ($\omega_{3,4}$) given by the negative difference of terms in bracket. For stability, we therefore require that the roots given by the positive sum in the brackets ($\omega_{1,2}$) are also purely imaginary. It may be shown that this condition reduces to

$$\frac{2}{3}\left(\frac{\rho_o}{r_o}\right)^3 + 3\left(\frac{z_o}{r_o}\right)^2 - 1 < 0 \tag{43}$$

with an equality in Eq. (43) defining the boundary between regions of stability and instability. With an equality, the solution of Eq. (43) is of the form $z_o = \lambda\rho_o$, with λ a constant. Substituting for z_o, λ can be obtained as the solution to

$$\tfrac{2}{3} + 3\lambda^2(1 + \lambda^2)^{\frac{1}{2}} - (1 + \lambda^2)^{3/2} = 0 \tag{44}$$

Numerically, it is found that $\lambda \doteq 0.442$, so that the configuration space is again partitioned into distinct regions of stability and instability, viz.,

1) $\rho_o < 2.26 z_o$: one real pair of roots ($\omega_{1,2}$) and one purely imaginary pair ($\omega_{3,4}$)—unstable; and

2) $\rho_o > 2.26 z_o$: two pairs of purely imaginary roots ($\omega_{1...4}$)—stable.

The partitioning is therefore defined by a cone, the section of which is shown in Fig. 2 as the line S_1.

General Synchronous Mode

For this mode of halo orbit, the roots of the characteristic polynomial, as defined by Eq. (32), may now be written as

$$\omega_{1\ldots4} = \pm\frac{\Omega_*}{\sqrt{2}}\left(\left[1-3\left(\frac{r_o}{r_*}\right)^3\right] \pm\left\{9\left[1-\left(\frac{r_o}{r_*}\right)^3\right]^2+36\left(\frac{r_o}{r_*}\right)^3\left(\frac{z_o}{r_o}\right)^2\right\}^{1/2}\right)^{1/2} \tag{45}$$

where $\Omega = r_*^{-3/2}$ is constant. A necessary condition for stability is that the term $1-(r_o/r_*)^3<0$, so that the region defined by $r_o<(1/3)^{1/3}r_*$ will be necessarily unstable. The determination of the overall stability map requires a numerical solution of Eq. (45). The section of the resulting boundary surface is shown as S_2 in Fig. 3, with the intersection of the surface with the ρ axis at the point $\rho_o = (1/3)^{1/3}r_*$.

It has been seen, then, that stable families of halo orbits exist for each of the halo modes. In the unstable regions, however, the time scale of the instability is long enough that a simple feedback control scheme will stabilize the trajectories. Numerical simulations using the full nonlinear equations of motion and a rotating Sun-line have confirmed this.

Patched Halo Trajectories

Now that the fundamental modes of operation of halo orbits have been established, the patching of halo orbits to form complex and elaborate new trajectories will be investigated. The patching process will be carried out by transferring from one halo orbit to another through a simple, assumed instantaneous, switching operation on the sail orientation. At each of these switching points, a number of boundary conditions must be satisfied to make the transfer possible. The conditions to be met are

1) $r_1 = r_2$: Intersection of the halo orbits.

2) $v_1 = v_2$: No velocity impulse required at switching point.

3) $E_1 = E_2$: Total sail energy is continuous across switching operation.

4) $\beta_1 = \beta_2$: Sail loading is continuous across switching operation.

Condition 1 ensures that the transfer is possible, while conditions 2–4 ensure that no other operation other than the switching of the sail orientation is required. As a consequence

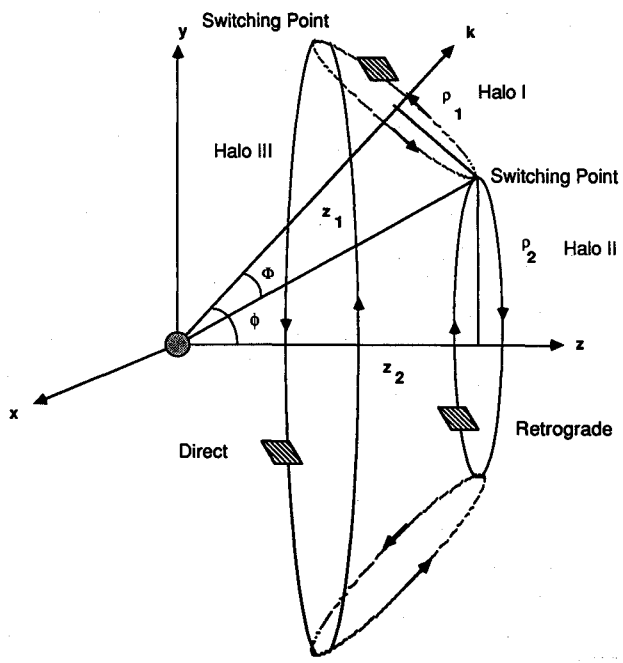

Fig. 5 Patched trajectories formed form off-axis and on-axis halo orbits.

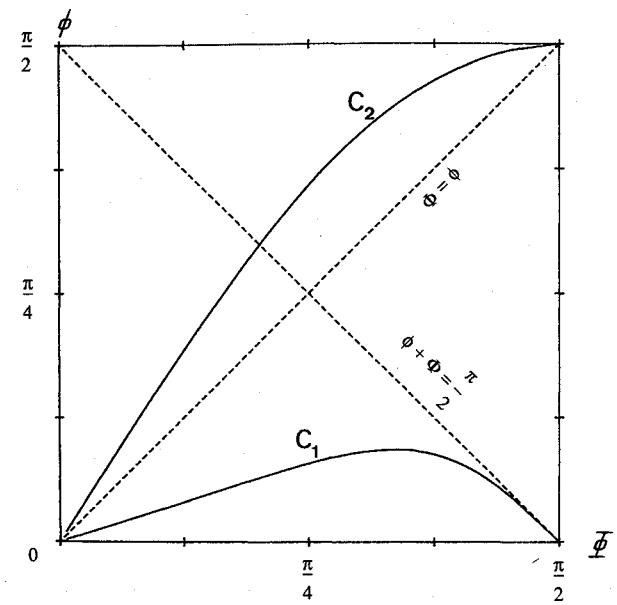

Fig. 6 Conditions for patching off-axis to on-axis halo orbits.

of condition 2, the halo orbits must intersect tangentially. It is clear, then, that the sail can only transfer to/from an off-axis halo (I) to an on-axis halo (II), or between two off-axis halo orbits. This transfer can occur at an upper or lower point on the off-axis halo (Fig. 5).

Since the switching operation is assumed to take place instantaneously, there is no change in the sail gravitational potential across the switching operation. Furthermore, since the radiation field potential is nonconservative with respect to rotations of the sail (i.e., no work is done against the field by reorienting the sail), condition 3 reduces to ensuring that $|v_1| = |v_2|$ (i.e., $\rho_1\Omega_1 = \rho_2\Omega_2$). This condition, therefore, determines the period of halo II as $\Omega_2 = \Omega_1\,(\rho_1/\rho_2)$.

Upper Transfer

First, the upper switching point will be considered with a transfer from the off-axis to the on-axis halo. Owing to the dynamic reversibility of the problem, the transfer can, of course, take place from the on-axis to the off-axis halo. The sail loadings required for each halo are given by Eqs. (13b) and (10b) as, using conditions 1–3,

$$\beta_1 = \frac{z_1}{r^3}\cos^{-2}\phi, \qquad \Omega_1 = \Omega_*, \qquad \alpha = \phi \tag{46a}$$

$$\beta_2 = \frac{z_2}{r^3}\left\{1+\left(\frac{\rho_2}{z_2}\right)\left[1-\left(\frac{\Omega_2}{\Omega_*}\right)^2\right]^2\right\}^{3/2}, \quad \Omega_2 = \Omega_*\left(\frac{\rho_1}{\rho_2}\right) \tag{46b}$$

with the sail orientation on halo II given by Eq. (10a). The sail loadings can be equated using condition 4 to obtain a function $\beta_1 - \beta_2 = 0$. This function can be reduced to two variables by eliminating (ρ_2,z_2), which are related to (ρ_1,z_1) through a rotation

$$\begin{Bmatrix}\rho_2\\ z_2\end{Bmatrix} = \begin{Bmatrix}\cos\phi & \sin\phi\\ -\sin\phi & \cos\phi\end{Bmatrix}\begin{Bmatrix}\rho_1\\ z_1\end{Bmatrix} \tag{47}$$

The resulting condition for a patched equal energy, equal loading trajectory then becomes $F_1(\phi,\Phi) = 0$, where

$$F_1(\phi,\Phi) = \cos^2\phi \times\left\{1+\tan^2(\phi+\Phi)\left[1-\cos^{-2}\phi\left(1+\frac{\tan\phi}{\tan\Phi}\right)^{-2}\right]^2\right\} -(1-\tan\phi\tan\Phi)^{-2/3}, \quad \tan\Phi = \frac{\rho_1}{z_1} \tag{48}$$

The numerical solution to this equation is shown in Fig. 6 as C_1 in the (ϕ,Φ) plane. It can be seen that $\phi + \Phi \leq (\pi/2)$, so that halo II always lies on the $+z$ (nightside) of the planet, as is required for the solution to be physical.

It should be noted that the system is rotationally symmetric about the z axis, so that the sail may transfer from halo II to halo I at any azimuthal position.

Lower Transfer

The analysis for the lower switching point is similar to that of the upper point, with the resulting condition $F_2(\phi,\Phi) = F_1(\phi, -\Phi) = 0$. The numerical solution is shown as C_2 in Fig. 6. The sail may transfer at will to and from halo I as it orbits on halo III, with halo III being retrograde with respect to halo I and halo II. It can be seen that there is no intersection of the curves in Fig. 6, so that it is not possible, with the imposed boundary conditions, to transfer at both the upper and lower switching points from the same initial off-axis halo orbit I.

Azimuthal Transfer

The possibility of patching together off-axis halo orbits will now be investigated. Consideration of the geometry shows that for condition 4 to hold, the off-axis angles ϕ must be equal. Then, for conditions 1-3 to hold, it is clear that the sail may only transfer onto neighboring off-axis halo orbits of the same amplitude and displacement. By then patching together these azimuthally neighboring halo orbits with on-axis halo orbits, extremely complex patched halo trajectories may be constructed.

Keplerian Transfer

The sail orientation may also be switched into a null configuration with $\alpha = \pi/2$, so that the sail is transferred onto a Keplerian orbit. This Keplerian orbit may be circular or elliptical, depending on the initial halo orbit.

Off-Axis Transfer

First a transfer to/from an off-axis halo I to a Keplerian ellipse will be considered. (It may be shown that condition 3 cannot be satisfied for transfer to a circular orbit.) The switching point may be either at the apogee or perigee of the ellipse and either at the upper or lower arc of the halo (Fig. 7). At these switching points, the perigee and apogee Keplerian velocities are given by

$$|v|_p = \left[\frac{1}{a}\left(\frac{1+e}{1-e}\right)\right]^{1/2}, \qquad |v|_a = \left[\frac{1}{a}\left(\frac{1-e}{1+e}\right)\right]^{1/2} \tag{49}$$

where (a,e) are the semimajor axis and eccentricity of the Keplerian ellipse. If we consider a transfer to/from the perigee, then, for condition 1 to be satisfied, the sail angular velocity on the off-axis halo must be $\Omega_* = r_p^{-3/2}$, where $r_p = a(1-e)$ is the perigee distance. Therefore, equating $|v|_p$ to the sail orbital velocity, $\Omega_*\rho_1$, to satisfy condition 3 we obtain the required halo amplitude

$$\rho_1 = a(1-e)\,(1+e)^{1/2} \tag{50}$$

Furthermore, since $\sin(\phi - i) = \rho_1/r_p$, we may obtain the required orientation of the off-axis halo

$$\phi = i + \sin^{-1}(1+e)^{1/2} \tag{51}$$

where i is the ecliptic inclination of the Keplerian ellipse. In particular, the sail may be transferred from an off-axis halo orbit onto a Keplerian polar orbit. A similar set of expressions are obtained for an apogee transfer [i.e., $\rho_1 = \rho_1(-e)$, $\phi = \phi(-e)$].

On-Axis Transfer

With this type of patched trajectory, the sail is transferred fom an on-axis halo orbit I to a Keplerian orbit, which may in this case be circular. The circular transfer is possible, since the sail angular velocity is now a free parameter, unlike the off-axis case, and can be chosen to satisfy the boundary conditions.

It can be seen from Fig. 7 that for a perigee transfer the halo amplitude and displacement are given in terms of the orbital elements of the ellipse by $\rho_1 = a(1-e)\sin(i)$, $z_1 = a(1-e)\cos(i)$. Therefore, to satisfy condition 3, the required sail angular velocity is given by

$$\Omega_1 = a^{-3/2}\sin^{-1}(i)\,\frac{(1+e)^{1/2}}{(1-e)^{-3/2}} \tag{52}$$

For an apogee transfer $\Omega_1(a,e,i) = \Omega_1(a,-e,i)$, and with $\Omega_1(a,0,i)$, the angular velocity for a transfer onto a circular orbit is obtained.

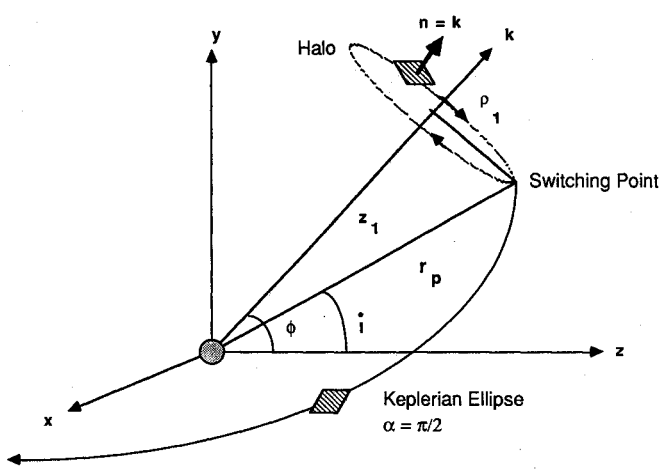

Fig. 7 Patching of an off-axis halo orbit to a Keplerian ellipse.

Conclusions and Applications

It is proposed that solar sails in halo orbits could be used on a planetary nightside to study its magnetotail and interaction with the solar wind. By patching such a halo orbit to a Keplerian ellipse, the sail could periodically sweep over the day-side to investigate the full three-dimensional structure of the magnetotail. Other applications include real-time stereographic investigation of a planetary surface when used either in a low displacement polar synchronous mode along with another spacecraft in near polar orbit, or with the sail on a low-displacement off-axis halo bringing it over the planetary day-side, again in conjunction with another spacecraft on a Keplerian orbit. Finally, these halo orbits demonstrate the unique ability of solar sails to execute trajectories and carry out missions impossible for any other spacecraft type.

Appendix

The sail characteristic acceleration is given by $a = P_o/\sigma$ so that the sail loading parameter (the sail characteristic acceleration required in units of the gravitational acceleration at $1R_o$) is related to the total sail mass per unit area by

$$\sigma(\mathrm{g}^{-2}) = C_j/\beta \tag{A1}$$

where the numerical constant is given by

$$C_1 = 1.62 \times 10^{-2}, \quad \text{Mercury} \tag{A2}$$

$$C_2 = 1.97 \times 10^{-3}, \quad \text{Venus} \tag{A3}$$

$$C_3 = 9.31 \times 10^{-4}, \quad \text{Earth} \tag{A4}$$

$$C_5 = 1.05 \times 10^{-3}, \quad \text{Mars} \tag{A5}$$

Acknowledgment

This work was carried out with the support of a Royal Society of Edinburgh Robert Cormack Fellowship (C.R.M.).

References

[1]McInnes, C. R., and Simmons, J. F. L., "Solar Sail Halo Orbits I: Heliocentric Case," *Journal of Spacecraft and Rockets,* Vol. 29, No. 4, 1992, pp. 466–471.

[2]McInnes, C. R., and Simmons, J. F. L., "Halo Orbits for Solar Sails—Dynamics and Applications," *ESA Journal,* Vol. 13, No. 3, pp. 229–234.

[3]Forward, R. L., "The Statite: A Non-Orbiting Spacecraft," AIAA Paper 89-2546, July 1989.

[4]Isayev, Y. N., and Kunitsyin, A. L., "To the Problem of Satellite's Perturbed Motion Under the Influence of Solar Radiation Pressure," *Celestial Mechanics,* Vol. 6, No. 3, 1972, pp. 44–51.

Alfred L. Vampola
Associate Editor